Adsorption Equilibrium Constants and Intraparticle Diffusivities in Molecular Sieves by Tracer-Pulse Chromatography

A perturbation chromatography technique using radiotracer gases has been developed to determine the adsorption equilibrium constants and diffusivities in molecular sieves. The ethane and ethylene 13X molecular sieve systems were studied in regions of high concentration. The data obtained by this technique are shown to be in agreement with equilibrium data obtained by static methods and with kinetic data obtained by adsorption uptake and chromatographic methods, but not with kinetic data obtained using NMR techniques. The tracer-pulse chromatographic technique is much more efficient for obtaining gas adsorption equilibria and intraparticle diffusivities and is considerably easier to adapt to wide pressure and temperature ranges than the conventional methods.

S. H. HYUN and R. P. DANNER

Department of Chemical Engineering
The Pennsylvania State University
University Park, PA 16802

SCOPE

Despite the obvious industrial importance of adsorption equilibria and kinetics in porous materials such as molecular sieves, reliable information in this area is still quite limited. This condition is the result of experimental difficulties and, in part, of the lack of a complete model to describe the complex adsorption kinetic process in porous solids. The adsorption kinetic or intraparticle diffusivity data reported in the literature have frequently shown discrepancies of several orders of magnitude among different investigators using different techniques of measurement.

Ruthven (1983) recently reviewed methods for determining diffusivities in zeolites. Most earlier studies used direct measurement of the adsorption uptake on an exposed layer of adsorbent. A chromatographic method is also being used which is based on the analysis of response of an adsorption bed to a concentration pulse or step change at the inlet. More recently NMR methods have been used to measure adsorption diffusivities. The chromatographic techniques are easier to operate, more efficient in producing data, and more suitable for higher temperature and pressure ranges. Conventional chromatographic methods, however, have been limited to infinitely dilute adsorbed phase concentrations with only one adsorbable component. Furthermore, Kärger and Ruthven (1981) have raised doubts about the micropore diffusivities determined by adsorption uptake and chromatographic techniques. Use of NMR for the study of adsorption diffusivities involves an extension of the methods originally developed to study self-diffusion in liquids. Application of NMR is restricted to molecules which contain a sufficiently high density of atoms with impaired nuclear spins, such as found with the hydrogens in hydrocarbons.

The objective of this work was to develop a tracer-pulse chromatographic technique (i.e., perturbation chromatography technique) which can be used for both pure and multicomponent systems over the entire concentration range. A mathematical model using bidispersed pore structure, which is more realistic in pelletized particles, has been developed to describe the chromatographic behavior of a tracer pulse. An analysis of the response of the adsorption column to a pulse of radiotracer gas is used to obtain adsorption equilibrium and kinetic data. The accuracies of the chromatographic model and the tracer-pulse techniques are examined on the basis of the pure-component adsorption data. Various aspects of the adsorption kinetics of ethane and ethylene in 13X molecular sieves are discussed.

CONCLUSIONS AND SIGNIFICANCE

The tracer-pulse technique can be a very useful method for determining adsorption equilibrium constants as well as the intraparticle mass transfer parameters. The tracer-pulse technique is not confined to infinitely dilute concentration ranges because the adsorption equilibrium constant is independent of the amount of tracer isotope injected. For any concentration of the adsorbed phase, the amount of isotope injected is usually so small that the assumptions of first-order kinetics for the mass transfer through the phase boundaries and of constancy of the intraparticle diffusivities inside the pulse boundary should be acceptable.

The first moment of the response peak to a small pulse of ra-

S. H. Hyun is currently at the College of Engineering, Yonsei University, Seoul, Korea.

dioactive gas was found to be independent of the adsorption rate parameters in the experimental systems studied. An effect of porosity on the first moment was observed. The adsorption equilibrium constants obtained from the first moments are in excellent agreement with those obtained from the proven static method.

Micropore tracer diffusivities for C_2H_4 and C_2H_6 in 13X molecular sieves were determined and found to range between 3×10^{-9} and 5×10^{-8} cm^2/s at 118 kPa and in the temperature range of 298 to 373 K. These values are in agreement with previously reported values based on adsorption uptake or chromatography. They disagree substantially, however, with values determined by NMR. This discrepancy may be caused by the differences in the zeolite crystals used in the different studies, inadequacy of the bidispersed model used to describe the molecular sieve pellets, or shortcomings in experimental techniques. Resolution of this difference will have to await additional data and analysis.

The macropore diffusivities of C_2H_4 and C_2H_6 in 13X molecular sieves are 5.9×10^{-2} to 7.3×10^{-2} cm^2/s depending on the temperature. No difference in the diffusivities of C_2H_4 and C_2H_6 in 13X molecular sieves was observed at the given temperature and pressure. The high values of the macropore diffusivities show that the diffusion process in the macropores of 13X molecular sieves is in the ordinary diffusion regime instead of the Knudsen regime.

The adsorption kinetics at low temperatures were found to be controlled by the micropore diffusion process in small particles (radius of 0.023 to 0.046 cm). In large particles (radius of 0.113 cm), however, the adsorption rate is governed by both the macro- and micropore diffusion processes, particularly at high temperatures. To determine the intraparticle diffusivities accurately, relatively small particles and high flow rates are preferred, as this minimizes the longitudinal dispersion effects.

INTRODUCTION

Early studies of sorption kinetics in porous particles were made using the direct measurement of sorption rates. More recently chromatographic and NMR techniques have been used. Barrer (1971) reviews earlier gravimetric and volumetric techniques and provides an excellent review of diffusion processes in crystalline zeolites. Antonson and Dranoff (1969) used an analysis of the chromatographic breakthrough curve to obtain intraparticle diffusivities in zeolites. Ruthven (1983) reviews these methods as well as the newer NMR approach.

Since the application of the principle of elution gas chromatography to the measurements of effective diffusion coefficients in porous solids was reported by Davis and Scott (1965), many authors have been interested in this method. In the beginning, the chromatography techniques were described by a simple model such as the Van Deemter equation based on a single pore diffusivity (Ma and Mancel, 1972). A more exact theory of chromatography which used a single pore model but analyzes the various mass transport steps in the packed column has been described by Kucera (1965) and Grubner (1968). The results based on using a single pore diffusivity, however, show that the observed diffusivity could be much greater than the macropore diffusivity but much less than the micropore diffusivity. The correct values of the diffusivities can not therefore be obtained.

A model for transient sorption in solids having bidispersed pore structures (i.e., macropores and micropores) was developed by Ruckenstein et al. (1971) and, slightly differently, by Sargent and Whitford (1971). Such a model is more realistic for describing sorption in pelletized particles and in some types of molecular sieves. Thus, most of the recent authors in the literature have accepted the bidispersed pore model in the chromatographic study of intraparticle diffusivities in molecular sieves (Shah and Ruthven, 1977; Chihara et al., 1978; Ruthven and Kumar, 1979; Andrieu and Smith, 1980; Hsu and Haynes, 1981).

The application of standard gas chromatography techniques to the measurement of intraparticle diffusion in porous solids is subject to serious limitations because of two critical assumptions: linearity of the equilibrium isotherm over the relevant concentration range, and independence of the micropore diffusivity on the adsorbed phase concentration. Furthermore, the usual chromatographic techniques are limited to infinitely dilute adsorbed phase concentrations with only one adsorbable component. On the other hand, the tracer-pulse method does not require such assumptions and can be extended to multicomponent systems as discussed by Hyun and Danner (1982b). Although the concentration-pulse method might also be applicable to higher concentration ranges, extending this method to multicomponent systems is impractical for studying adsorption kinetics of the individual components since it is not possible to separate the individual component diffusivities from the overall rate coefficient determined by the concentration-pulse technique. Therefore, this paper focuses on the tracer-pulse technique which appears to be the most promising of the available methods.

THEORY

The transport of gas molecules in a packed bed takes place according to complex steps. Each step influences the rate of mass transfer inside the porous particles and thus contributes to the band-broadening of the chromatographic zone. By analyzing the contributions of each step to the shape of a chromatographic response peak, adsorption kinetic parameters in porous particles can be determined. A model for determining the mass transport parameters in molecular sieves by the tracer-pulse techniques has been developed using the basic concepts of Kucera (1965) and Ruckenstein et al. (1971).

In this model, an adsorbent particle tableted from small crystals or fine powder is assumed to include relatively large pores (macropores) consisting of voids between the crystals and small pores (micropores) within the crystals themselves. The adsorbent particle is assumed spherical for reasons of simplicity, and uniformly interspersed with macropores. The pore structure is continuous and interconnecting. The same arguments are applied to the micropores within the crystal. In the tracer-pulse experiments at constant total pressure, the velocity of the mobile phase is constant because there is no sorption effect. This issue was discussed by Hyun and Danner (1982b). The model equations for the bidispersed pores are summarized below.

For the mass balance in the bulk gas phase:

$$-D_L \frac{\partial^2 C^*}{\partial z^2} + U \frac{\partial C^*}{\partial z} + \frac{\partial C^*}{\partial t} = Q_A \tag{1}$$

$$C^*(0,t) = \frac{M}{F}\,\delta(t) \tag{2}$$

$$C^*(z,0) = 0, \quad z > 0 \tag{3}$$

$$\lim_{z \to \infty} C^*(z,t) = 0, \quad t > 0 \tag{4}$$

For the diffusion in the macropore:

$$\frac{\partial C_A^*}{\partial t} - D_A\left(\frac{\partial^2 C_A^*}{\partial r_A^2} + \frac{2}{r_A}\frac{\partial C_A^*}{\partial r_A}\right) = Q_B + Q_{AA} \tag{5}$$

$$C_A^*(z,r_A,0) = 0 \tag{6}$$

$$\left.\frac{\partial C_A^*}{\partial r_A}\right|_{r_A=0} = 0 \tag{7}$$

$$Q_A = -\frac{3\epsilon_A D_A}{\epsilon_e R_A}\left.\frac{\partial C_A^*}{\partial r_A}\right|_{r_A=R_A} \tag{8}$$

For the diffusion in the micropore:

$$\frac{\partial C_B^*}{\partial t} - D_B\left(\frac{\partial^2 C_B^*}{\partial r_B^2} + \frac{2}{r_B}\frac{\partial C_B^*}{\partial r_B}\right) = Q_c \tag{9}$$

$$C_B^*(r_B,z,0) = 0 \tag{10}$$

$$\partial C_B^*/\partial r_B|_{r_B=0} = 0 \tag{11}$$

$$Q_B = -\int_{-\infty}^{\infty}\left.\frac{3\epsilon_B D_B}{\epsilon_A R_B}\frac{\partial C_B^*}{\partial r_B}\right|_{r_B=R_B} \cdot f(R_B)d\ln(R_B) \tag{12}$$

For the mass transfer through the boundary film on the particle:

$$Q_A = -H_A(K_A C^* - C_A^*|_{r_A=R_A}) \tag{13}$$

$$Q_B = -H_B(K_B C_A^* - C_B^*|_{r_B=R_B}) \tag{14}$$

For the mass transfer through the film at the pore wall and adsorption on the solid surface:

$$Q_{AA} = -H_{AA}(K_{AA}C_A^* - C_{AA}^*) \tag{15}$$

$$Q_c = -H_c(K_c C_B^* - C_{BA}^*) \tag{16}$$

$$Q_{AA} = -\partial C_{AA}^*/\partial t \tag{17}$$

$$Q_c = -\partial C_{BA}^*/\partial t \tag{18}$$

$$C_{AA}^*(z,r_A,0) = 0 \tag{19}$$

$$C_{BA}^*(z,r_B,0) = 0 \tag{20}$$

The model which the above equations describe includes a number of assumptions. While these assumptions are not valid in most conventional chromatographic techniques, they are acceptable for the tracer-pulse technique. It is a good assumption that the adsorption equilibrium constant of the tracer isotope is identical to that of the unlabeled species already equilibrated with the adsorbent, independent of the amount of tracer isotope injected. For any concentration of the adsorbed phase, the amount of isotope injected is usually so small that the assumption of first-order kinetics for the mass transfer through the boundaries should be acceptable. By the same token, the constancy of the intraparticle diffusivities can be assumed. There are no thermal effects caused by the adsorption since the adsorption of the solute isotopes is considered to be simply a self-exchange of solute molecules. On the other hand, in conventional chromatographic techniques all of these assumptions can be critical even in the Henry's law region (Hsu and Haynes, 1981; Ruthven, 1977, 1983). Therefore, for accurate study of the dependency of the intraparticle diffusivities on adsorbed phase concentrations, among all the chromatographic methods available at present only the tracer-pulse technique should be used. Other assumptions incorporated in the model are negligible pressure drop across the column and plug flow. (The experimental pressure drop across every column used in this study was found to be negligible.) Furthermore, it is assumed that the effects of nonplug flow through the column are adequately described by a longitudinal dispersion coefficient, and such effects through the pore channels are negligible since these channels are very small capillaries.

An exact solution of the set of Eqs. 1 to 20 has not been attempted. Since the response peak of a tracer pulse has a lot of background noise, a curve-fitting method using the exact analytical solution may be less accurate and more complex than the moment analysis method. The moment analysis method up to the second moment can successfully be applied to estimate model parameters from the nearly Gaussian curves observed in the tracer-pulse technique. In this study, therefore, only the solution in the Laplace domain required for the moment analysis was obtained.

A well-known relation between moments in the time domain and derivatives in the Laplace domain can be used to calculate the ordinary moments of the response curves (Levenspiel and Bischoff, 1963). The procedure for obtaining the moment equations requires extremely complex and tedious calculations and thus is not reproduced here (see Hyun, 1982). The resultant moment equations for the first absolute moment, μ_1' (i.e., retention time), and the second central moment, μ_2 (i.e., the variance), are:

$$\mu_1' = \frac{L}{U}\left\{1 + K_A\left[\frac{\epsilon_A}{\epsilon_e}(K_{AA}+1) + \frac{\epsilon_B}{\epsilon_e}K_B(K_c+1)\right]\right\} \tag{21}$$

$$\mu_2 = \frac{2D_L L}{U^3}(1 + K_A\phi_1 K')^2 + \frac{2L}{U}K_A\phi_1\left\{\frac{K'^2 R_A^2}{15D_A} + \frac{K_{AA}}{H_{AA}} + \frac{K'^2}{H_A}\phi_1 + K_B\phi_2\left[\frac{(K_c+1)^2}{15D_B}\int_{-\infty}^{\infty}R_B^2 f(R_B)d\ln(R_B) + \frac{K_c}{H_c} + \frac{(K_c+1)^2}{H_B}\phi_2\right]\right\} \tag{22}$$

where:

$$K' = K_{AA} + 1 + \phi_2 K_B(K_c+1) \tag{23}$$

$$\phi_1 = \epsilon_A/\epsilon_e \tag{24}$$

$$\phi_2 = \epsilon_B/\epsilon_A \tag{25}$$

The model developed up to this point is for the very general case, and thus the moment equations are very complex. For a particular system, the model can be simplified by the introduction of appropriate assumptions.

The model assumes that both a gas phase and an adsorbed phase exist in the micropores. Adsorption on microporous adsorbents such as zeolites, however, is usually considered as micropore filling since the molecules adsorbed in micropores are never free from force fields associated with the pore wall. Therefore, the concept of single-phase adsorption is preferable in molecular sieves. For this case, the adsorption equilibrium constant on the micropore surface can be regarded as zero. In general, for physical adsorption the sorption rate constants on the pore surfaces approach infinity. Additionally, in the infinitely dilute concentration range of the tracer solute the mass transfer resistance between the boundaries can be assumed to be negligible, compared with the diffusional resistance in the macropores and micropores. For these concentration ranges, the phase equilibrium constant between the bulk gas phase and the gas phase in the macropores is assumed to be unity because the molecular sizes of the tracer components investigated are relatively small in comparison with the macropore openings. Thus:

$$K_c = 0 \tag{26}$$

$$H_A = H_B = H_{AA} = H_c = \infty \tag{27}$$

$$K_A = 1.0 \tag{28}$$

Substituting these conditions into Eqs. 21 and 22, one obtains:

$$\mu_1' = \frac{L}{U}(1 + \phi_1 K) \tag{29}$$

$$\sigma^2 = \mu_2 = \frac{2D_L L}{U^3}(1 + \phi_1 K)^2 + \frac{2L}{U}\phi_1\left[\frac{K^2R_A^2}{15D_A} + K_B\phi_2 \cdot \frac{1}{15D_B}\int_{-\infty}^{\infty} R_B^2 f(R_B)d\ln(R_B)\right] \quad (30)$$

where:

$$K = K_{AA} + 1 + \phi_2 K_B \quad (31)$$

In this simplified model, the first moment depends only on the interstitial flow velocity, the adsorption equilibrium constants in the macropores and micropores, and the various porosities. The second moment depends on the interstitial velocity, the macro- and micropore diffusivities, the adsorption equilibrium constants, and the characteristics of the column.

By rearranging Eq. 30, a useful equation for measuring the mass transfer parameters is obtained:

$$\frac{\sigma^2 U}{2L} = \frac{D_L}{U^2}(1 + \phi_1 K)^2 + \frac{\epsilon_A}{\epsilon_e}\frac{K^2R_A^2}{15}\frac{1}{D_A} + \frac{\epsilon_B}{\epsilon_e}\frac{K_B}{15D_B}\int_{-\infty}^{\infty} R_B^2 f(R_B)d\ln(R_B) \quad (32)$$

Equations 29 and 30 have forms similar to those found in the literature (Chihara et al., 1978; Andrieu and Smith, 1980; Shah and Ruthven, 1977). Since detailed information about the microparticle size distribution in the 13X molecular sieves used in this experiment was not available, the log-normal size distribution function was replaced with the average crystal size of NaX.

Using Eqs. 29 and 32, the mass transfer parameters D_L, D_A, and D_B can be calculated from properly selected experimental data. If the retention time, $\bar{t}_R$, and the second moment, σ^2, are determined at various flow rates and the retention times are plotted as a function of L/U, a straight line should be obtained according to Eq. 29. The slope of the straight line, S_1, is:

$$S_1 = 1 + \phi_1 K \quad (33)$$

or

$$K = \frac{\epsilon_e}{\epsilon_A}(S_1 - 1) = K_{AA} + 1 + \phi_2 K_B \quad (34)$$

From Eq. 34, the adsorption equilibrium constants K_{AA} and K_B can be obtained.

If the experimental data $\sigma^2U/2L$ are plotted versus $1/U^2$, the intercept at infinite velocity, I_1, becomes:

$$I_1 = (\epsilon_A/\epsilon_e)(K^2R_A^2/15D_A) + (\epsilon_B/\epsilon_e)(K_BR_B^2/15D_B) \quad (35)$$

The intercept I_1 gives the contribution of the internal pore diffusion resistance, which is independent of the flow velocity. To eliminate the porosity effect on the micropore diffusion term for different columns, the intercepts are divided by ϵ_B/ϵ_e, and then K is replaced using Eq. 34:

$$I_1\left(\frac{\epsilon_e}{\epsilon_B}\right) = \frac{(S_1 - 1)^2}{15D_A}\left(\frac{\epsilon_e^2}{\epsilon_A\epsilon_B}\right)R_A^2 + \frac{K_BR_B^2}{15D_B} \quad (36)$$

If these intercepts for different particle sizes are determined, and $I_1(\epsilon_e/\epsilon_B)$ values are plotted against R_A^2, a straight line should be obtained, provided that $(S_1 - 1)^2/15D_A \cdot (\epsilon_e^2/\epsilon_A\epsilon_B)$ is independent of R_A. From the intercept of this straight line at the zero particle size, I_2, the micropore diffusivity, D_B, can be obtained.

$$I_2 = \frac{K_BR_B^2}{15D_B} \quad (37)$$

The macropore diffusivity, D_A, can be calculated from the slope, S_2, of the plot of $I_1(\epsilon_e/\epsilon_B)$ vs. R_A^2 since from Eq. 36:

TABLE 1. PHYSICAL PROPERTIES OF 13X MOLECULAR SIEVES

Surface area*	420 m^2/g
Apparent density	2.31 g/cm^3
Pellet density	1.215 g/cm^3
Micropore volume*	0.24 cm^3/g
Macropore volume	0.15 cm^3/g
Average crystal radius of NaX	1.5×10^{-4} cm

* 80% of the NaX values.

$$S_2 = \frac{(S_1 - 1)^2}{15D_A}\left(\frac{\epsilon_e^2}{\epsilon_A\epsilon_B}\right) \quad (38)$$

or

$$D_A = \frac{(S_1 - 1)^2}{15}\left(\frac{\epsilon_e^2}{\epsilon_A\epsilon_B}\right)R_A^2 \Big/ \left[I_1\left(\frac{\epsilon_e}{\epsilon_B}\right) - \frac{K_BR_B^2}{15D_B}\right] \quad (39)$$

EXPERIMENTAL

The apparatus and operating procedure have been described in detail by Hyun (1982) and Hyun and Danner (1982b). A numerical integrating method was used to determine the moments of the tracer response peaks. The first and second moments needed in the moment analysis must be those relating only to the adsorption column; i.e., excluding the contributions of the system dead volume, the injection and detection time, and other extracolumn effects. For strongly adsorbed gases and a long column these extraneous contributions can be neglected, particularly in the second moment. In this study, however, these side effects were eliminated by using a bypass column which had negligible gas volume. Subtracting the moments of the bypass peaks from those of the adsorption peaks through the column gave the desired corrected moments. For the given flow rate and characteristics of the column, no pulse-size effect on the moments was observed. This result is quite consistent with the theoretical predictions from the model assumptions and Eqs. 29 and 30.

The adsorbate gases used were research grade ethane (99.99%) and ethylene (99.95%). The adsorbent used was 13X molecular sieves with 20% binder manufactured by the Linde Division of the Union Carbide Corporation (Lot No. 13945390174). The details of the physical properties of 13X molecular sieves are given in Table 1. The radioisotopes of ethane $C_2^{14}H_6$, manufactured by New England Nuclear Company and of ethylene $C_2^{14}H_4$, manufactured by Amersham Corp., were diluted with pure ethane and ethylene, respectively, and then used as tracer samples. After dilution, the concentration of the radioisotopes was 20.7 millicurie per gmol of ethane and 25. 2 millicurie per gmol of ethylene.

A number of adsorption columns were prepared in this study to investigate effects of the properties of the packed column on the first and second moments of the response peaks. The characteristics of three of these columns are given in Table 2. The essential difference between these columns was the size of the packed particles; i.e., the particle diameter to column diameter ratio at constant column diameter. For the purpose of clarity, these columns are hereafter referred to as the 1/10, 1/5, and 1/2 columns, based on the particle diameter to column diameter ratio.

RESULTS AND DISCUSSION

Adsorption Equilibrium Constant

First moment data were collected on 13X molecular sieves at a constant total pressure of 118 kPa and temperatures of 298 and 373 K for C_2H_6, and temperatures of 298, 323, and 373 K for C_2H_4. The flow rates varied from 20 cm^3/min to 150 cm^3/min (298 K, 101.3 kPa). First moment data in the 1/10 column are shown in Figure 1 as an example.

According to Eq. 29, the first moment must be a linear function of L/U with a slope of $(1 + \phi_1 K)$. The experimental data sets

TABLE 2. ADSORPTION COLUMN CHARACTERISTICS

Characteristics	1/10 Column	1/5 Column	1/2 Column
Column:			
Diameter, cm	0.4826	0.4826	0.4826
Cross sectional area, cm^2	0.1829	0.1829	0.1829
Packed Bed:			
Length, cm	14.37	14.37	14.61
Volume, cm^3	2.628	2.628	2.6725
Adsorbent:			
Mass packed, g	1.5284	1.5420	1.427
Avg. particle radius, cm	0.023	0.046	0.1113
Column length/dia. ratio	30	30	30
Particle dia./column dia. ratio	1/10	1/5	1/2
Volume fraction of column (column porosity)			
Interparticle, ϵ_e	0.505	0.517	0.561
Solid phase, ϵ_s	0.261	0.254	0.231
Macropore, ϵ_A	0.0896	0.088	0.080
Micropore, ϵ_B	0.1444	0.141	0.128

TABLE 3. ADSORPTION EQUILIBRIUM CONSTANTS OF ETHANE AND ETHYLENE ON 13X MOLECULAR SIEVES AT 118 kPa

Adsorbate	Column	T, K	Adsorption Equilibrium Constant, K_B: From Tracer-Pulse Data	From Static Data
C_2H_4	1/10	298	247.0	246.0
		323	237.0	235.0
		373	185.0	185.0
	1/5	298	232.0	246.0
		323	218.0	235.0
		373	161.8	185.0
	1/2	298	248.0	246.0
		323	238.0	235.0
		373	195.0	185.0
C_2H_6	1/10	298	198.0	197.0
		373	95.0	92.0
	1/5	298	176.0	197.0
		373	75.0	92.0
	1/2	298	201.0	197.0
		373	98.0	92.0

substantiate this theoretical requirement. The interstitial velocity, U, is the velocity at the column temperature and pressure which was obtained by dividing the volume flow rate at the column conditions by the cross-sectional area available for gas flow. The slopes of the straight lines depend on the column fractions of each phase in the column and the adsorption equilibrium constants K_{AA} and K. Therefore, the slopes for a given gas at the same temperature are different depending on the column. From these linear relationships it is concluded that no nonequilibrium effects exist in the given ranges of flow rate.

Assuming the adsorption equilibrium constant on the macropore surface, K_{AA}, to be negligible in comparison with the micropore adsorption equilibrium constant, K_B, is equivalent to assuming that adsorption on 13X molecular sieves is based on the filling of the micropores. With this assumption, K_B can be directly determined from the slope of the plot of $\bar{t}_R$ vs. L/U and the known column volume fractions given in Table 2. The adsorption equilibrium constants for C_2H_4 and C_2H_6 13X molecular sieve systems were calculated and are given in Table 3. This table also includes the adsorption equilibrium constants determined from the static data of Hyun and Danner (1982a) at the same conditions as those in this work.

The adsorption equilibrium constant, K_B, is independent of the particle size of 13X molecular sieves and thus should have constant values for every column at a fixed temperature and pressure. In the cases of the 1/10 and 1/2 columns, which were packed with the smallest and the largest particles, respectively, almost identical equilibrium constants were obtained. These adsorption equilibrium constants are also in excellent agreement with those calculated from the static data. The values obtained by the tracer-pulse method in the 1/5 column, however, are as much as 20% too low compared to the other two columns and the static data. This is believed to be a result of experimental error in the sample preparation. The equality of the adsorption equilibrium constant obtained by the two methods means that the assumption that $K_{AA} = 0$ is valid for the adsorption of C_2H_4 and C_2H_6 on 13X molecular sieves in the ranges of pressure and temperature studied.

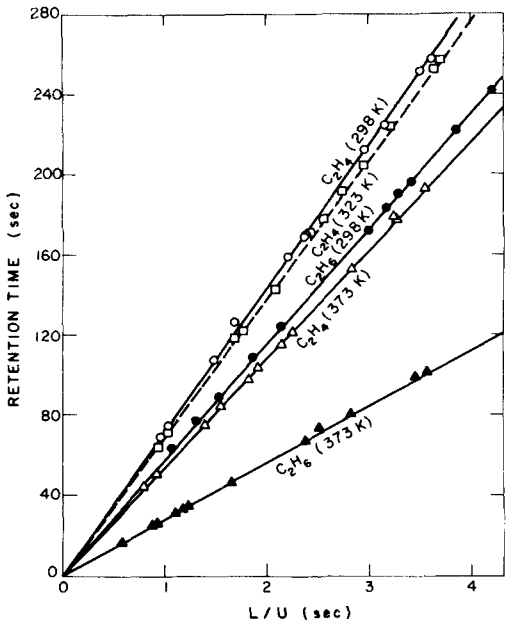

Figure 1. First moments in the 1/10 column (R_A = 0.023 cm) at 118 kPa.

Micropore Diffusivity

The second central moments, σ^2, were also obtained from the tracer-pulse peaks. Figure 2 is an example plot of $\sigma^2 U/2L$ vs. $1/U^2$

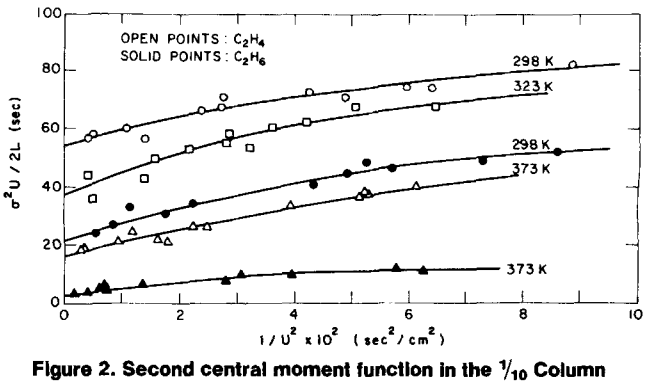

Figure 2. Second central moment function in the 1/10 Column (R_A = 0.023 cm) at 118 kPa.

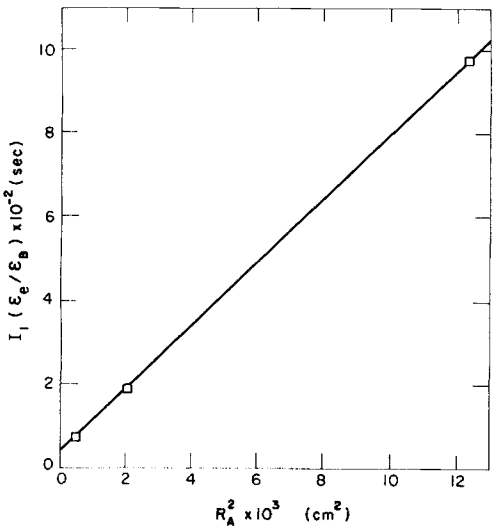

Figure 3. Dependencies of intraparticle diffusion resistances of ethane on particle sizes of 13X molecular sieves at 118 kPa and 298 K.

for the C_2H_4 and C_2H_6 systems at different temperatures in the 1/10 column. Since the tracer-pulse peaks had a lot of background noise, the exact determination of the second moment was difficult and resulted in some scattering of the data. The intercept, I_1, at infinite velocity in this type of plot includes the macropore and micropore diffusion contributions. The intercepts were determined graphically for every system from the smooth curves interconnecting the experimental data points. Equation 32 shows that the intercept, I_1, strongly depends on the adsorbent particle size as well as the microparticle size. While the particle size did change, the microparticle size is assumed to be the zeolite crystal size, and thus does not vary. Therefore, the dependency of the intercept on the particle size is caused predominantly by the macropore diffusion resistance. As the particle size increased, an increase in the intercept was observed. This effect will be discussed later. The second moments obtained in the 1/5 column include the same experimental errors as those involved in the determination of the adsorption equilibrium constants because the same response peaks were used. The inaccuracy of the adsorption equilibrium constant is directly projected on the values of $\sigma^2U/2L$ as can be seen in Eq. 32.

The values of $I_1(\epsilon_e/\epsilon_B)$ for ethane at 118 kPa and 298 K are plotted against R_A^2 in Figure 3 as an example. Using the intercepts of these linear plots at zero particle size, I_2, the micropore diffusivities of the tracer ethylene at 298, 323, and 373 K and of the tracer ethane at 298 K and 373 K on 13X molecular sieves were determined at 118 kPa by Eq. 37. The adsorption equilibrium constant, K_B, was taken as the average of those in the 1/10 and 1/2 columns at each temperature. These data are given in Table 4. The micropore tracer diffusivities were found to be between 3.2×10^{-9} and 4.8×10^{-8} cm^2/s. The micropore diffusivity is a strong function of the molecular size and the concentration of the adsorbed phase. Since C_2H_4 and C_2H_6 have similar molecular sizes, molecular size effects could not be observed in this study. The concentration dependence of the micropore diffusivities can be more clearly expressed in terms of the fractional coverage, θ, of the adsorbent instead of pressures or adsorbed phase concentrations. The fractional coverage was calculated by dividing the amount adsorbed at the given temperature and pressure by the limiting amount of adsorption. The limiting amounts of adsorption (Table 4) were calculated from the vacancy solution model (Suwanayuen and Danner, 1980). The amounts adsorbed for C_2H_4 and C_2H_6 on 13X molecular sieves at the given conditions were given by Hyun and Danner (1982a). To clarify the dependency of the micropore adsorption on the fractional coverages, a further study under various concentrations at the constant temperature would be required. From the variation of the diffusivities with temperatures at constant coverage, the activation energy for the micropore diffusion can be determined at the specified concentration.

Recently there have been several papers published comparing micropore diffusivities determined by adsorption techniques and NMR methods (Kärger et al., 1980; Kärger and Ruthven, 1981; Ruthven, 1983). In general these authors report considerable discrepancies between the diffusivities determined by the previous adsorption and NMR methods. Kärger and Ruthven suggest that these differences are caused primarily by failure to account properly for the effects of external heat and mass transfer resistance and by the use of different zeolite crystals. With careful attention to these possible causes of discrepancies, Kärger and Ruthven found good agreement between the uptake adsorption method and the NMR method for C_3H_8 and C_4H_{10} in 5Å molecular sieve and for triethylamine in 13X molecular sieve. For benzene in 13X molecular sieve however, they report large discrepancies: $\simeq10^{-8}$ – 10^{-9} cm^2/s by adsorption uptake and $\simeq10^{-6}$ cm^2/s by NMR at 250 K. These measurements were made under apparently similar conditions on samples from the same original batch of molecular sieve. The authors suggest that this difference might be caused by small differences in the adsorbent regeneration procedures or some other unidentified shortcomings in the experimental procedures or models.

A number of authors have reported adsorption uptake and chromatographic diffusivity values for systems similar to those in our work. For C_2H_6 in 4Å molecular sieve at 298 K reported diffusivities range from 4×10^{-12} to 6×10^{-13} cm^2/s (Kondis and Dranoff, 1971; Eagan and Anderson, 1975; Antonson and Dranoff, 1969). Those for C_2H_6 in 5Å molecular sieve at 298 K range from 6×10^{-12} to 3×10^{-10} cm^2/s (Antonson and Dranoff, 1969; Derrah, 1973; Shah and Ruthven, 1977). Since 13X molecular sieve has larger pore windows than 5Å molecular sieve, the micropore diffusivity of C_2H_6 in 13X molecular sieve should be larger than the value in 5Å molecular sieve, as found in the present study.

Kärger et al. (1980) determined the micropore diffusivity of C_2H_6 in a NaX zeolite at 300 K to be between 10^{-4} and 10^{-5} cm^2/s

TABLE 4. PORE DIFFUSIVITIES OF TRACER ISOTOPES ON 13X MOLECULAR SIEVES AT 118 KPA

Adsorbate	T, K	Limiting Amt. Adsorbed $\times 10^3$ kmol/kg	Coverage θ	Micropore $D_B\times10^8$, cm^2/s	Macropore $D_A\times10^2$, cm^2/s	Molecular Self $D_m\times10^2$, cm^2/s	Internal Tortuosity τ_{in}
C_2H_4	298	2.98	0.94	0.32	5.9	10.9	1.85
	323	2.84	0.77	0.45	6.5	12.7	1.95
	373	2.77	0.56	1.2	7.2	16.7	2.32
C_2H_6	298	2.52	0.82	0.76	5.7	9.1	1.60
	373	3.85	0.32	4.8	7.3	14.2	1.95
						Average =	1.93

depending on the loading of the adsorbent. This range is quite different from the 10^{-8} to 10^{-9} cm^2/s range found by us using the tracer-pulse method and from the other values cited above. Kärger and Ruthven (1981) and Lee and Ruthven (1977) suggest that these low values from the adsorption method are caused by failure to properly account for heat dissipation and external diffusional resistance or by differences between the zeolite crystals.

In the tracer-pulse adsorption method there is no question regarding thermal effects since equilibrium (pressure and concentration, as well as temperature equilibrium) is maintained throughout the analysis. The molecular sieve samples used by Kärger et al. (1980) and us, however, were quite different. Kärger et al. used high-purity, laboratory-prepared crystals while those used in our study were commercial grade crystals pelletted with a 20% by weight clay binder. Other causes of the discrepancy should also be considered. We characterized our particle size in terms of a mean average particle size rather than a particle size distribution. Hsu and Haynes (1981) have reported that the value of the diffusivity based on the mean particle size is about two orders of magnitude smaller than the true value. Further consideration of the bidispersed pore model itself may be required. The possibility of a combined rate-limiting effect caused by the micropore diffusion and the external mass transfer resistance might be considered. Finally, further consideration of concentration effects may be required. Most of the other data reported in the literature are in the Henry's law region rather than in the high concentration region of the present study.

The resolution of the discrepancy between the NMR and tracer-pulse diffusivity values will have to await further data and analysis. In any case, the tracer-pulse method provides an efficient and potentially effective means of determining micropore diffusivities.

Macropore Diffusivity

The macropore diffusivities of the tracer C_2H_4 and C_2H_6 isotopes in 13X molecular sieves at 118 kPa were calculated at several temperatures using Eq. 38. The macropore diffusivities for these systems are presented in Table 4.

The values of the macropore diffusivities range from 5.7×10^{-2} to 7.3×10^{-2} cm^2/s. These values are 3 to 4 times as large as the Knudsen diffusion coefficients calculated approximately from the Knudsen equation (Satterfield, 1970). Considering the relatively large macropores in 13X molecular sieves, the diffusion of small molecules in these pores may occur by the ordinary diffusion mechanism rather than by Knudsen diffusion. These diffusivities increase slowly with temperature in a manner similar to molecular diffusivities, while the micropore diffusivities change rapidly with temperature. The macropore diffusivities obtained in this study are the macropore tracer diffusivities at the infinitely dilute concentrations of the radioisotopes in the macropores. These are independent of the adsorbed phase concentration, assuming that the adsorption in the macropores is negligible. The data confirm this argument because C_2H_6 and C_2H_4 have almost identical macropore diffusivities at the same temperature and pressure. Since the macropore size is very large in comparison with the molecular sizes of C_2H_6 and C_2H_4, the dependency of the molecular size on the macropore diffusivity would be negligible. In general, the macropore diffusivity depends on the bulk molecular diffusivity and the internal tortuosity inside the macropores.

In order to compare the macropore diffusivity with the bulk molecular diffusivity, the molecular self-diffusivities of C_2H_4 and C_2H_6 at 118 kPa and the given temperatures are shown in Table 4. These were calculated from the Wilke and Lee modification of the Hirschfelder equation. The molecular self-diffusivities of C_2H_4 are slightly higher than those of C_2H_6. In order to obtain a relationship between the molecular diffusivity and the macropore diffusivity, the internal tortuosity in the macropores must be considered. The diffusion path length in the macropores is larger than the distance along a straight line in the mean direction of diffusion. The tortuosity factor is defined as the ratio of the former length to the latter. The diffusion flux prediced by the equations for ordinary diffusion for the straight diffusion path must be corrected by an internal tortuosity factor to be related to the macropore diffusivity. Internal tortuosities, however, should be independent of the diffusing gas and be characteristic of the geometry of the porous adsorbent. Therefore, the above argument for nearly equal macropore diffusivities for C_2H_4 and C_2H_6 is reasonable since they have approximately equal molecular self-diffusivities. Satterfield (1970) suggested a relationship between the bulk gas diffusivity and the effective pore diffusivity. This relationship can be simplified for the macropore diffusion since the macropores are relatively large in comparison with the molecular sizes of the diffusing gases. Furthermore, the macropore diffusion was found to occur by the ordinary diffusion mechanism in this study. The simplified relationship is:

$$D_A \approx D_m/\tau_{in} \tag{40}$$

The internal tortuosities, τ_{in}, in the macropores were calculated by Eq. 40 and are given in Table 4. The difference between them is probably caused by the assumption that every column used for determining the macropore diffusivity had the same tortuosity. Although the tortuosity is not constant, the average value, $\tau_{in} = 1.93$, is quite reasonable when compared to other values in the literature. Roberts and York (1967), Sargent and Whitford (1971), and Lee and Ruthven (1977) obtained around 2.0 for τ_{in} in molecular sieve pellets. Somewhat higher values (3 to 5) in beds of carbon particles were reported by Andrieu and Smith (1980).

Adsorption Kinetics on 13X Molecular Sieves

In order to examine the mechanism of the adsorption kinetics of C_2H_6 and C_2H_4 on 13X molecular sieves, the micropore and macropore diffusion time constants, D_B/R_B^2 and D_A/R_A^2, were determined from the data given in Table 4. In general, the macropore diffusion time constants are 800 to 65 times as large as those for the micropore in the 1/10 column, 200 to 15 times those for the 1/5 column, and 35 to 3 times those for the 1/2 column; see Table 5. The maximum difference between the macropore and micropore time constants occurs at the lowest temperature. The large values of D_A/R_A^2 in comparison with D_B/R_B^2 in the 1/10 and 1/5

TABLE 5. MICROPORE AND MACROPORE DIFFUSION TIME CONSTANTS ON 13X MOLECULAR SIEVES AT 118 KP A

Adsorbate	T, K	D_B/R_B^2, s^{-1}	Column	D_A/R_A^2, s^{-1}
C_2H_4	298	0.14	1/10	112
			1/5	27.9
			1/2	4.8
	323	0.20	1/10	123
			1/5	30.7
			1/2	5.2
	373	0.53	1/10	136.0
			1/5	34.0
			1/2	5.8
C_2H_6	298	0.34	1/10	108.0
			1/5	26.9
			1/2	4.6
	373	2.13	1/10	138
			1/5	34.5
			1/2	5.9

TABLE 6. RELATIVE CONTRIBUTIONS OF THE LONGITUDINAL DISPERSION, MACROPORE DIFFUSION RESISTANCE, AND MICROPORE DIFFUSION RESISTANCE ON 13X MOLECULAR SIEVES AT 118 kPa

Column	Adsorbate	T, K	U, cm/s	Total $\frac{\sigma^2 U}{2LS_1^2}$ s	Long. Disp. $\frac{D_L}{U^2}$ s	Macro. Diffusion $\frac{\epsilon_B(S_1-1)^2R_A^2}{15\epsilon_A S_1^2 D_A}$ s	Micro. Diffusion $\frac{\epsilon_B K_B R_B^2}{15\epsilon_e S_1^2 D_B}$ s
1/10	C_2H_4	298	4.53	0.014	0.0043	0.0033	0.0064
		323	4.87	0.013	0.0052	0.0030	0.0048
		373	4.37	0.013	0.0078	0.0027	0.0025
	C_2H_6	298	4.36	0.015	0.0082	0.0034	0.0034
		373	4.16	0.015	0.0114	0.0025	0.0011
1/2	C_2H_4	298	4.65	0.117	0.0143	0.0949	0.0078
		323	4.74	0.100	0.0082	0.0860	0.0058
		373	4.40	0.088	0.0082	0.0771	0.0027
	C_2H_6	298	4.31	0.125	0.0230	0.0975	0.0041
		373	4.47	0.091	0.0170	0.0729	0.0012

columns indicate that the adsorption of C_2H_6 and C_2H_4 on 13X molecular sieves at 298 and 323 K can be explained by micropore diffusion-controlled kinetics. For the cases in the 1/2 column, however, this type of interpretation is not uniformly true. For example, the micropore diffusion time constant of C_2H_6 at 373 K in the 1/2 column is almost one-third of its macropore diffusion time constant. In this case, the adsorption kinetics are governed by both the macro- and micropore diffusion processes. As shown in Table 5, the contribution of the macropore diffusion process to the adsorption kinetics becomes more significant as the particle size or temperature increases.

An evaluation of the contribution of each mass transfer parameter to the dispersion of the response peak is very helpful in understanding the dynamic behaviors of adsorbate gases in a chromatographic column. Each contribution can be clearly perceived using the following expression instead of Eq. 32:

$$\frac{\sigma^2 U}{2LS_1^2} = \frac{D_L}{U^2} + \frac{\epsilon_e (S_1-1)^2}{\epsilon_A \quad S_1^2} \frac{R_A^2}{15D_A} + \frac{\epsilon_B}{\epsilon_e} \frac{K_B}{S_1^2} \frac{R_B^2}{15D_B} \qquad (41)$$

In this equation, the first, second, and third terms are the contributions of the longitudinal dispersion, the macropore diffusion resistance, and the micropore diffusion resistance, respectively. The relative contributions of these are given in Table 6. The flow rates were arbitrarily selected within the range of flow rates usually used in adsorption equilibrium studies.

The most important point in Table 6 is that there are significant differences in the macropore diffusion resistances between the 1/10 and 1/2 columns. For example, the percentage of the macropore diffusion resistance for C_2H_6 at 373 K is only 17% in the 1/10 column but 80% in the 1/2 column. The major contribution to the dispersion in the 1/2 column arises from the macropore diffusion resistance, being larger than 78% of the total dispersion for every system. In comparison with these contributions, micropore diffusion contributes to the dispersion by less than 7%, thus being almost negligible. In the 1/10 column, however, all three contributions are important except for the cases at 373 K. At higher temperatures, the contribution of the longitudinal dispersion becomes more important; i.e., 60% for C_2H_4 and 76% for C_2H_6 at 373 K. As the particle diameter to column diameter ratio decreases, the contributions of the micropore diffusion and the longitudinal dispersion show predominant importance. The absolute values of the micropore diffusion resistance, however, are almost independent of the particle diameter to column diameter ratio.

From the above observations, it is evident that to obtain accurate dispersion coefficients small particles of the absorbent as well as gases with a small molecular diameter must be used to eliminate the macropore and micropore contributions. On the other hand, small particles and high flow rates are preferred for studying the intraparticle diffusion, since in this way the longitudinal dispersion effects can be minimized. If the longitudinal dispersion coefficient and the macropore diffusivity can be estimated by appropriate correlations, the micropore diffusivity can be determined from a single experimental response peak using Eq. 32. This method does not require multiple data points in various columns with differing particle sizes. In order to obtain micropore diffusivities from a single experimental peak, another experimental study on the longitudinal dispersion behavior would be required.

ACKNOWLEDGMENT

The authors wish to thank D. M. Ruthven for his thoughtful comments and suggestions. Support of the National Science Foundation under Grant No. CPE-8012423 is gratefully acknowledged.

NOTATION

C^* = concentration of radioactive component i in mobile phase, mol/cm^3
C_A^* = concentration of radioactive component i in macropores, mol/cm^3
C_{AA}^* = concentration of radioactive component i on macropore surface, mol/cm^3
C_B^* = concentration of radioactive component i in micropores, mol/cm^3
C_{BA}^* = concentration of radioactive component i on micropore surface, mol/cm^3
D_A = effective macropore tracer diffusivity, cm^2/s
D_B = effective micropore tracer diffusivity, cm^2/s
D_L = effective longitudinal dispersion coefficient, cm^2/s
D_m = molecular diffusivity, cm^2/s
F = volumetric flow rate of mobile phase at column conditions, cm^3/s
$f(R_B)$ = normal particle size distribution function
H_A = mass transfer rate constant through stationary film between bulk gas phase and macropores, s^{-1}
H_{AA} = adsorption rate constant on macropore surface, s^{-1}
H_B = mass transfer rate constant through boundary film between macropore and micropore, s^{-1}
H_c = adsorption rate constant on micropore surface, s^{-1}
I_1 = quantity defined by Eq. 35
I_2 = quantity defined by Eq. 37

K = quantity defined by Eq. 31
K' = quantity defined by Eq. 23
K_A = phase equilibrium constant between bulk gas phase and gas phase in the macropores
K_{AA} = adsorption equilibrium constant on macropore surface
K_B = phase equilibrium constant between gas phase in macropores and micropores
K_c = adsorption equilibrium constant on micropore surface
L = length of column, cm
M = moles of radioactive isotopes injected
Q_A = mass transfer rate through film between bulk gas phase and gas phase in macropores, mol/cm^3 s
Q_B = mass transfer rate through boundary between macropores and micropores, mol/cm^3 s
Q_{AA} = mass transfer rate through boundary at macropore wall, mol/cm^3 s
Q_c = mass transsfer rate through boundary at micropore wall, mol/cm^3 s
r_A = radial distance from center of particles, cm
r_B = radial distance from center of microparticles, cm
R_A = radius of adsorbent particles, cm
R_B = radius of adsorbent crystals (microparticles), cm
S_1 = quantity defined by Eq. 33
S_2 = quantity defined by Eq. 38
t = time or elution time, s
t_R = retention time, s
U = interstitial mobile phase velocity at column conditions, cm/s
z = axial distance from column inlet, cm

Greek Letters

ϵ = total porosity of column
ϵ_A = macropore volume fraction of total column volume
ϵ_B = micropore volume fraction of total column volume
ϵ_e = interparticle volume fraction of total column volume
ϵ_s = solid volume fraction of total column volume
τ_{in} = internal tortuosity factor in macropores
θ = fractional coverage of limiting amounts of adsorption
μ_1' = absolute first moment, s
μ_2 = second central moment, s^2
σ^2 = variance, s^2
ϕ_1 = quantity defined by Eq. 24
ϕ_2 = quantity defined by Eq. 25
$\delta(t)$ = delta function at inlet at time zero

LITERATURE CITED

Andrieu, J., and J. M. Smith, "Rate Parameters for Adsorption of CO_2 in Beds of Carbon Particles," *AIChE J.*, **26**, 944 (1980).

Antonson, C. R., and J. S. Dranoff, "Adsorption of Ethane on Type 4A Molecular Sieve Particles," *Chem. Eng. Prog. Symp. Ser.*, No. 96, 27 (1969).

Barrer, R. M., "Intracrystalline Diffusion," *Adv. Chem. Ser.*, **102**, 1 (1971).

Chihara, K., M. Suzuki, and K. Kawazoe, "Adsorption Rate on Molecular Sieving Carbon by Chromatography," *AIChE J.*, **24**, 237 (1978).

Davis, B. R., and D. S. Scott, "Measurement of the Effective Diffusivity of Porous Pellets," 58th Ann. Meet. AIChE, Philadelphia (Dec., 1965).

Derrah, R. I., "Diffusion in Molecular Sieve Zeolites," Ph.D. Thesis, Univ. of New Brunswick, Fredericton, NB (1973).

Eagan, J. D., and R. B. Anderson, "Kinetics and Equilibrium of Adsorption on 4A Zeolite," *J. Colloid Interface Sci.*, **50**, 419 (1975).

Grubner, O., "Statistical Moments Theory of Gas-Solid Chromatography: Diffusion-Controlled Kinetics," *Adv. in Chromatog.*, **6**, 173 (1968).

Hsu, L. K. P., and H. W. Haynes, Jr., "Effective Diffusivity by the Gas Chromatography Technique: Analysis and Application to Measurements of Diffusion of Various Hydrocarbons in Zeolite NaY," *AIChE J.*, **27**, 81 (1981).

Hyun, S. H., "Adsorption of Azeotropic Binary Gas Mixtures on Molecular Sieve Type 13X," M.S. Thesis, Pennsylvania State Univ., University Park, PA (1980).

———, "Gas-Mixture Adsorption Isotherms and Diffusivities in Molecular Sieves by Perturbation Chromatography," Ph.D. Thesis, Pennsylvania State Univ., University Park, PA (1982).

Hyun, S. H., and R. P. Danner, "Equilibrium Adsorption of Ethane, Ethylene, Isobutane, Carbon Dioxide, and Their Mixtures on 13X Molecular Sieves," *J. Chem. Eng. Data*, **27**, 196 (1982a).

———, "Determination of Gas Adsorption Equilibria by the Concentration-Pulse Technique," *AIChE Symp. Ser.*, **78** (219), 19 (1982b).

Kärger, J., et al., "Self-Diffusion of *n*-Paraffins in NaX Zeolites," *J. Chem. Soc.*, Faraday Trans. I, **76**, 717 (1980).

Kärger, J., and D. M. Ruthven, "Diffusion in Zeolites," *J. Chem. Soc.*, Faraday Trans. I, **77**, 1,485 (1981).

Kondis, E. F., and J. S. Dranoff, "Kinetics of Isothermal Sorption of Ethane on 4A Molecular Sieve Pellets," *Ind. Eng. Chem. Proc. Des. Dev.*, **10**, 108 (1971).

Kucera, E., "Linear Non-Equilibrium Elution Chromatography," *J. Chromatog.* **19**, 237 (1965).

Lee, L. K., and D. M. Ruthven, "An Experimental Method for the Determination of Macropore Diffusivities in Molecular Sieve Pellets," *Ind. Eng. Chem. Fund.*, **16**, 290 (1977).

Levenspiel, O., and K. B. Bischoff, "Patterns of Flow in Chemical Process Vessels," *Adv. Chem. Eng.*, **4**, 95 (1963).

Ma, Y. H., and C. Mancel, "Diffusion Studies of CO_2, NO, NO_2, and SO_2 on Molecular Sieve Zeolites by Gas Chromatography," *AIChE J.*, **18**, 1,148 (1972).

Roberts, P. V., and R. York, "Adsorption of Normal Paraffins from Binary Liquid Solutions by 5A Molecular Sieve," *Ind. Eng. Chem. Proc. Des. Dev.*, **6**, 516 (1967).

Ruckenstein, E., A. S. Vaidyanathan, and G. R. Youngquist, "Sorption by Solids with Bidispersed Pore Structures," *Chem. Eng. Sci.*, **26**, 1,305 (1971).

Ruthven, D. M., "Diffusion in Molecular Sieves: A Review of Recent Developments," *ACS Symp. Ser.*, **40**, 320 (1977).

———, "Diffusion in A, X, and Y Zeolites," *ACS Symp. Ser.*, **218**, 345 (1983).

Ruthven, D. M., and I. H. Doetsch, "Diffusion of Hydrocarbons in 13X Zeolite," *AIChE J.*, **22**, 882 (1976).

Ruthven, D. M., and R. Kumar, "A Chromatographic Study of the Diffusion of N_2, CH_4 and Binary CH_4-N_2 Mixtures in 4A Molecular Sieve," *Can. J. Chem. Eng.*, **57**, 342 (1979).

Ruthven, D. M., and L. K. Lee, "Kinetics of Nonisothermal Sorption: Systems with Bed Diffusion Control," *AIChE J.*, **27**, 654 (1981).

Sargent, R. W. H., and C. J. Whitford, "Diffusion of Carbon Dioxide in Type 5A Molecular Seive," *Adv. Chem. Ser.*, **102**, 155 (1971).

Satterfield, C. N., *Mass Transfer in Heterogeneous Catalysis*, M.I.T. Press, Cambridge, MA (1970).

Shah, D. B., and D. M. Ruthven, "Measurement of Zeolitic Diffusivities and Equilibrium Isotherms by Chromatography," *AIChE J.*, **23**, 804 (1977).

Suwanayuen, S., and R. P. Danner, "A Gas Adsorption Isotherm Equation Based on Vacancy Solution Theory," *AIChE J.*, **26**, 68 (1980).

Manuscript received Oct. 31, 1983; revision received July 16, 1984 and accepted July 23.